

Accepted Manuscript

Effects of Forced Convection on the Performance of a Photovoltaic Thermal System: An Experimental study

Alibakhsh Kasaeian, Yasamin Khanjari, Soudabeh Golzari, Omid Mahian, Somchai Wongwises

PII: S0894-1777(17)30041-9

DOI: <http://dx.doi.org/10.1016/j.expthermflusci.2017.02.012>

Reference: ETF 9014

To appear in: *Experimental Thermal and Fluid Science*

Received Date: 8 September 2016

Revised Date: 8 February 2017

Accepted Date: 13 February 2017

Please cite this article as: A. Kasaeian, Y. Khanjari, S. Golzari, O. Mahian, S. Wongwises, Effects of Forced Convection on the Performance of a Photovoltaic Thermal System: An Experimental study, *Experimental Thermal and Fluid Science* (2017), doi: <http://dx.doi.org/10.1016/j.expthermflusci.2017.02.012>

This is a PDF file of an unedited manuscript that has been accepted for publication. As a service to our customers we are providing this early version of the manuscript. The manuscript will undergo copyediting, typesetting, and review of the resulting proof before it is published in its final form. Please note that during the production process errors may be discovered which could affect the content, and all legal disclaimers that apply to the journal pertain.



Effects of Forced Convection on the Performance of a Photovoltaic Thermal System: An Experimental study

Alibakhsh Kasaeian¹, Yasamin Khanjari¹, Soudabeh Golzari¹, Omid Mahian²,
Somchai Wongwises^{3,*}

¹Department of Renewable Energies, Faculty of New Science and Technologies, University of Tehran, Tehran, Iran.

²Young Researchers and Elite Club, Mashhad Branch, Islamic Azad University, Mashhad, Iran.

³Fluid Mechanics, Thermal Engineering and Multiphase Flow Research Lab. (FUTURE), Department of Mechanical Engineering, Faculty of Engineering, King Mongkut's University of Technology Thonburi, Bangmod, Bangkok 10140, Thailand.

*Corresponding author: somchai.won@kmutt.ac.th

Abstract

A photovoltaic thermal system (PV/T) is a combination of solar cells and solar heating systems that simultaneously produces electricity and low-grade heat. The present paper experimentally investigates the effects of forced convection on the thermal and electrical efficiencies of a single-pass air PV/T system. For this purpose, a modified air-cooled PV/T system that is equipped with four fans to produce forced convection conditions was tested. The effects of air mass flow rate and depth of the channel were studied. The results illustrate that the reduction in the depth of air channel increases the thermal efficiency, but it has no considerable effect on the electrical efficiency. With increasing the mass flow rate of air, the thermal efficiency is increased, but a slight enhancement is obtained for the produced electrical power by PV. The outcomes show that the thermal efficiency of system with 0.05 (m) channel depth and air mass flow rate of 0.018 (kg/s) to 0.06 (kg/s) is approximately in the range of 15%–31% while the electrical efficiency just changes in the range of 12%–12.4%.

Keywords: PV thermal system; forced convection, thermal efficiency; air-cooled PV/T

NOMENCLATURE

A	Area	Subscript	
Aa	Cross section of channel area	a	air
Cp	Specific heat capacity(kJ/kgK)	amb	ambient
G	Solar radiation intensity(W/m ²)	abs	Absorber plate
I	Circuit current(A)	bs	back surface of tedlar
\dot{m}	Air mass flow rate(kg/s)	c	solar cell
Nu	Nusselt number	el	electrical
P	Power(W)	in	inlet
PV	Photovoltaic	mp	maximum power point
\dot{Q}	Heat transfer rate	oc	open-circuit
T	Temperature	out	outlet
V	Circuit Voltage(V), Wind speed(m/s)	ov	overall
	Greek Symbols	PV	Photovoltaic panel
δ	duct depth	sc	short-circuit
η	efficiency	th	thermal
ρ	Density(kg/m ³)		

1. Introduction

Photovoltaic panel converts a small part of solar energy into electricity, and the rest is wasted as heat and reflection. This may lead to increase the temperature of the cell and decrease the electrical efficiency. Circulation of a cold fluid such as water or air around the panel prevents from electrical efficiency drop. PV/T system is a combination of photovoltaic panel and solar thermal collector, in which both electrical and thermal energy produced at the same time [1]. Air and water are the most common fluids in PV/T collector systems. Since 1970's when Kern and Russell have introduced the main concepts of PV/T systems [2], various studies have been carried out on PV/T systems [3],[4]. The air-cooled PV/T collector has been more considered in terms of easy construction and less production cost [5],[6],[7],[8]. The simplest PV/T air collector design consists of a photovoltaic panel that is attached to an air duct. Other designs of PV/T air collectors are as single-pass or double-pass air flow, glazed or unglazed, using fins, metal sheets or channels in the duct [9],[10].

As mentioned before, the main concept of PV/T is to use the heat loss of the PV panels. Some of the common thermal applications of air PV/T systems include space heating, natural ventilation of buildings, and air preheating in industrial sites. Dehumidification of air in cabins, garages, allotment houses and mobile homes can also be mentioned as examples of PV/T applications [11],[12].

The building-integrated PVT system (BIPVT) can be extensively utilized in the roof or façade, in which air circulate around the PV cells. The hot air can be installed on wall or room to heating the space of one or more rooms. It can be passive or active. It is also can be used to warm the commercial buildings and factory sites. The other application of hot air is agriculture drying process. According to the usage of hot air, the mass flow rate and its temperature should be controlled [13],[12].

Researchers have studied PV/T systems using experimental and numerical methods [14],[15],[16],[17],[18]. In the last decade, many studies have been implemented to improve the efficiency of these systems and evaluate their economic and environmental aspects [19],[20],[21]. The performance of unglazed PV/T system was evaluated for various climatic conditions by Tiwari et al. [22] in Delhi, India. They concluded that the overall efficiency increased by 18% due to the utilization of thermal energy gathering in the system. Tonui and Tripanagnostopoulos [23] investigated the effect of using a thin flat metal sheet in the middle of air channel or finned back wall in glazed and unglazed PV/T air collector. Also, a numerical model was represented and validated against experimental data. The results showed that fins enhance the efficiency of the system. At the meantime, they carried out experiments to examine the performance of PV/T collector circulated with either forced or natural airflow [24]. In 2008 and 2009, Raman and Tiwari [25, 26] considered the energy and exergy efficiency of the PV/T air collector in five different climatic places. They also evaluated the performance of single-pass and double-pass air PV/T systems. They found that the double-pass PV/T system reaches a better performance than the single-pass type. Joshi et al. [27] studied and compared the performance of unglazed glass-to-glass and glass-to-temlar air PV/Ts, in different climatic places in New Delhi, India. They completed their investigation with validation versus the experimental data literature. The obtained results indicated that the glass-to-glass type had higher efficiency in comparison to the glass-to-temlar systems. Solanki et al. [28] experimented a PV/T solar heater system in an indoor testing process. They measured dependent factors by changing mass flow rate of air and solar intensity in steady state conditions. Ameri et al. [29] built a direct-coupled PV/T air collector in Kerman, Iran. Polycrystalline silicon PV panels were used. The power of fans was supplied directly from the PV

panels. They found that the amount of air mass flow rate is dependent on solar radiation and ambient temperature which varies with weather changes. According to the electrical energy consumption of fans, they presented the optimized velocity of air in the channel. Shahsavari et al. [30] considered the energy and exergy performance of the previous system (represented by Ameri et al. [29]) for both glazed and unglazed air PV/T types. They improved the performance with adding thin metal sheet in the middle of the air channel. They found that the exergy efficiency of the unglazed one was improved. Jin et al. [31] investigated the effect of adding rectangular tunnel absorber on the efficiency of a single pass solar collector system. Also, they tested different mass flow rates to observe the changes in the performance.

Bambrook and Sproul [7] evaluated the performance of an unglazed air PV/T system experimentally. They noted that using large ducts reduce the pressure drop and fan consumption power. Agrawal and Tiwari [32] carried out a comparative analysis of three types of air PV/Ts. They observed that the overall annual thermal energy and exergy gain of unglazed hybrid PV/T tiles was greater than others. Ji et al. [33] made a new design of tri-functional PV/T system. This model can be used with both air and water according to the needs of the seasonal and climatic conditions. The results indicate that in the air mode with the air mass flow rate of 0.04 (kg/s) leads in average electrical and thermal efficiencies of 10.2% and 46%, respectively. Kim et al. [34] studied an unglazed air PV/T system consisting of a mono-crystalline PV module experimentally. The average thermal and electrical efficiencies of the mentioned system had been achieved by 22% and 15 %, respectively.

The present paper aims to investigate the effects of forced convection created by four fans on the performance of an air-cooled PV/T system in the weather conditions of Tehran, Iran. The experiments are conducted for different values of air mass flow rates and depth of channel.

2. Description of the system

The photograph and a schematic picture of proposed experimental setup which is an air PV/T system with single pass channel are shown in Fig.1. The electrical section consists of two monocrystalline PV modules in a dimension of 1053×554 (mm), made by Aria Solar Co. in Iran. The PV panels are connected in series configuration. The electrical properties of PV panels given by the manufacturer are shown in Table 1. A steel plate with the dimensions of $2000 \times 500 \times 3$ (mm) was used as the thermal absorber and attached to the panels by aluminum oxide paste with thickness of 3 (mm). One of the advantages of using steel beside aluminum oxide paste is the reduction of cost. The thermal resistance of aluminum oxide paste and metal plate are $1.0909 \times 10^{-4} \left(\frac{K}{W}\right)$ and $6.3424 \times 10^{-5} \left(\frac{K}{W}\right)$, respectively. The air channel walls were made of

Plexiglas with a thickness of 4 (mm). By using some small pieces of Plexiglas holders on the channel walls, the channel depth could be set in three amounts of 5, 10 and 15 cm, according to Fig. 2. For testing each depth, the channel bottom plate was set on the desired depth. Then, the channel is sealed to prevent the air leakage. During the tests, the PV/T system is tilted in the latitude of Tehran towards the south. In the forced convection mode, the mass flow rate of air in the duct could be adjusted with four DATECH 1238-12HBIA- fans whose rated voltage and current are 12(v) and 1.5(A), respectively. The velocity of the air passing through the channel can be set in a range of 0.5 (m/s) to 2.5 (m/s) by changing the voltage of the fans. In fact, the speed and power of fans were controlled by changing the input voltage. By setting the fan speeds in four different amounts from 0.5 (m/s) to 2 (m/s) and three different channel depths, the air mass flow rate can be varied from 0.018 to 0.154 (kg/s).

The global radiations are measured by using a Hukseflux type-SR12 pyranometer. The pyranometer must be located parallel to the PV surface. Hotwire anemometer YK-2004AH was used to record the air flow velocity in the channel. The wind speed is recorded by the AM-4220 anemometer. The temperature of the panels' back surface was measured by thermocouples type-K and read by thermometer type TM-946. Fifteen SMT160 sensors were used to measure the temperatures. Seven of them measure the temperature of the absorber plate and five of them measure the temperature of the top surface of the panels. Three SMT160 sensors measured the temperatures of the inlet air, outlet air and ambient. All the sensors and the pyranometer were connected to a data logger. Two multimeters of type VICTOR VC97 were used to report the electrical data values (current, voltage of PV panels and fan power). Also, a variable resistance of 50 (Ω) was utilized to calculate the maximum power produced by the PV panels. The range of measurement and the accuracy of the experimental monitoring equipment are outlined in Table 2.

3. Experimental procedure

Outdoor experiments were carried out in the campus of the University of Tehran. The data were collected on the sunny days of August and September 2013 from 9:00 to 17:00 in Tehran. The latitude and longitude of Tehran are 35° 41' N and 51° 25' E, respectively. In Table 3, the performance of the air PV/T system was considered with the channel depth of 5 (cm), tilt angle of 35° and mass flow rate of 0.06 (kg/s). The solar intensity and the temperatures of the ambient, the inlet air, the outlet air were recorded and monitored. The average temperature of absorber plate, the back surface of the panel and the top surface of the panel is also measured. Beside the obtained results of thermal section, the electrical data such as the short circuit current, the open circuit voltage and the current and voltage in the maximum power were recorded and reported in Table 3.

4. Calculations

In order to focus on the performance of the PV/T system, two important parameters are introduced: thermal efficiency and electrical efficiency.

4.1. Electrical efficiency

The mathematical relation for calculation of electrical efficiency from measured test data is presented in Eq.(1) [2, 24, 29-31, 34-36]. All parameters involved in this equation were measured in current experiment. The maximum output power is obtained by multiplying the corresponding values of current and voltage as can be seen in Eq.(2).

$$\eta_{el} = \frac{P_{mp}}{A_{PV} \times G} \times 100 \quad (1)$$

$$P_{mp} = I_{mp} \times V_{mp} \quad (2)$$

The current and voltage is measured by a multimeter, utilizing variable resistances (loads) and I-V characteristic curve.

4.2. Thermal efficiency

The thermal efficiency expression is calculated from measured test data as follows [2, 23, 24, 29-31, 33-35]:

$$\eta_{th} = \frac{\dot{m}C_p(T_{out} - T_{in})}{A \times G} \quad (3)$$

where \dot{m} and C_p are the mass flow rate and specific heat capacity of the coolant, T_{in} and T_{out} are the coolant temperatures at the inlet and outlet, respectively. A is the collector aperture area and G is the incident solar irradiance normal to surface. The mass flow rate can be calculated by:

$$\dot{m} = \rho V_a A_s \quad (4)$$

A_s is the cross section area of channel, V_a is the velocity of fluid in the channel and ρ is the fluid density passing the channel.

4.3. Overall efficiency

The overall efficiency of the system is calculated with the following equation[2, 27, 33, 36]:

$$\eta_{ov} = \eta_{th} + \frac{\eta_{el}}{\eta_{cp}} \quad (5)$$

where the electrical efficiency is converted to an equivalent of thermal efficiency using electric power generation efficiency, η_{cp} for a conventional power plant. The value of η_{cp} depends on the power plant efficiency. Also, the value of η_{cp} varies between 0.30 and 0.40 in the literature. It is taken to be 0.40 in this experiment.

5. Results and discussion

The climatic conditions including solar irradiance and ambient temperature on 10th September 2013 are represented in Fig.3. In this figure, the daily variations of solar intensity from 9:00 to 17:00 are shown for the setup tilt angle of 35°. The value of solar intensity at noon, between 12:15 to 14:15 has been slightly changed, while in the early or late hours, it varies dramatically. The maximum value of solar intensity was between 980 (W/m²) and 1027 (W/m²). The ambient temperature changed between 32 (°C) to 38 (°C) during the day. The thermal and electrical performances of the system on this day are illustrated in Figs. 4 to 8.

In Fig.4 temperature variations of inlet and outlet air of channel are indicated. Also, the average temperature of absorber plate, the back surface of PV panel and the top surface of PV panel are shown in this figure. Some part of absorbed solar irradiance is converted into electricity and the rest part is conducted to absorber plate and finally transferred to air passing channel. There is also a significant heat loss due to the radiation and convection heat transfer from the top surface of panels. The back surface of the panel has the maximum value of temperature among the mentioned parts. This value would even reach up to 62 (°C).

The temperatures of inlet air and outlet air in the channel rise during the day. As the value of solar intensity rises in middle hours of the day, the temperature difference between inlet and outlet air in the channel also increases. The temperature of the absorber plate in the midday hours reaches to 56 (°C).

In Fig.5, the thermal efficiency of the system during a day is reported. As solar intensity increases at noon, in constant mass flow rate, the temperature difference between the air inlet and the air outlet the channel grows; consequently, the thermal efficiency values increase. The daily thermal efficiency on average is about 31%.

The daily variations of open circuit voltage, short circuit current, voltage and current in the maximum power point are illustrated in Figs. 6 and 7. The currents are significantly affected by

solar irradiance; so that by increasing the solar intensity, the currents grow at noon. Obviously, the currents are reduced in the afternoons when the solar radiation values fall. Unlike the currents, the voltages are in the maximum values in the early and late hours of a day. By increasing the temperature of the panel in the middle hours of a day, the values of voltages decrease.

The I-V characteristic curves for the hours 9:30, 13:15 and 16:30 are plotted in Fig.8. As the solar irradiance is reduced, the current of panel decreases.

The variation of the maximum power generation of photovoltaic panels versus time is shown in Fig. 9. According to Fig.8, each point in this curve is obtained by a change in variable resistance in the circuit for reaching the maximum electrical power output. The maximum electrical power output occurred at 13:15. The electrical efficiency of the system during the day is represented in Fig. 9 as well.

The thermal efficiency of the PV/T collectors was conventionally calculated as a function of the reduced temperature, which is defined as[2, 24, 34]:

$$T^* = \frac{\Delta T}{G} = \frac{T_{in} - T_{amb}}{G} \quad (6)$$

The thermal efficiency, η_{th} , is expressed as:

$$\eta_{th} = \eta_0 - \alpha \left(\frac{\Delta T}{G} \right) \quad (7)$$

Where η_0 is the thermal efficiency at zero reduced temperature, and α is the heat loss coefficient. Fig.10 illustrates the thermal efficiency with reduced temperature from the measured test data of the PV/T system. Fig.10 shows the data of the thermal efficiency at the time interval in which the collector is at or near normal incidence conditions.

The thermal efficiency of the air PV/T system can be represented by the following correlation:

$$\eta_{th} = 0.3357 - 19.61 (\Delta T / G).$$

The collector thermal efficiency at zero reduced temperature is 33% while the overall heat loss coefficient is 19.61 (W/m²K).

Then, the effect of the channel depth and the air mass flow rate are checked. The air mass flow rate can be varied in four different fan speeds from 0.5 (m/s) to 2 (m/s). In the Fig.11, the electrical, thermal and overall efficiencies are indicated for channel depth of 5 (cm) in different mass flow rate values. These results were obtained at the noon. In a constant depth of the channel, as the speed of the air passing through the channel and subsequently, Reynolds number increases, the flow regime changes from laminar to turbulent. This change will result in a remarkable improvement of convection heat transfer; therefore, the amount of the heat absorbed by the fluid

increases. Finally, the thermal efficiency grows significantly with increasing the air mass flow rate in constant channel depth. By increasing the mass flow rate in the range of 0.018 to 0.06 (kg/s) and Reynolds number in the range of 3100 to 10500, the overall efficiency grows to 45% and 61%, respectively.

In Fig.12, the variations of electrical efficiency versus air mass flow rate in different channel depths are shown. As mentioned before, the velocity of the air flowing in the channel can be set in the range of 0.5 (m/s) to 2.5 (m/s) by changing the voltage of the fans. Therefore, in three different channel depth of 5, 10 and 15 (cm), the air mass flow rate is obtained in range of 0.018 to 0.154 (kg/s). The change in the channel depth does not have a notable effect on the electrical efficiency. However, decreasing the channel depth increases the thermal efficiency. In constant mass flow rates, the larger channel depth causes the bigger cross sectional area. Consequently, the velocity of the air passing the channel decreases and the convection heat transfer coefficient will be reduced. This will cause reducing the channel outlet air temperature. Thus, as it can be seen in Fig.13, the increase in the channel depth will result in thermal efficiency drop. With the mass flow rate of 0.06 (kg/s), by reducing the channel depth from 15 to 5 (cm), the increase in the thermal efficiency would be 50% while a slight excess is observed for the electrical efficiency.

The most appropriate value for thermal efficiency in the channel depth of 5 (cm) and mass flow rate of 0.06 (kg/s) is about 31%. This value of efficiency was obtained by 19.25 (W) electrical power consumed by the fan.

The variations of the overall efficiency versus air mass flow rate are shown in Fig. 14. As it can be observed, the overall efficiency is further affected by the thermal efficiency rather than the electrical efficiency. Increasing of mass flow rate in the mentioned range causes 36% enhancement of the overall efficiency. Also, by decreasing the channel depth from 0.15 to 0.05 (m), an increment of 20% is obtained for the overall efficiency.

It is useful to compare the results of this study with the previous experimental or theoretical works. Joshi et al. [27] reported thermal and electrical efficiencies in the range of 13.4%-16.5% and 9.5%-11%, respectively. The glass-to-temlar unglazed air PV/T system studied by Joshi et al. didn't have absorber plate. Air with a mass flow rate of 0.05 (kg/s) flows directly beneath the PV panel in a duct with a depth of 0.05 (m). Sarhaddi et al. [36] studied an unglazed air PV/T system without absorber plate with 0.05 (m) channel depth. They achieved 25% thermal efficiency and 10% electrical efficiency using the mass flow rate of 0.06 (kg/s). In the other experimental research, an unglazed air PV/T system with the air channel depth of 0.06 (m) and without absorber plate was studied by Kim et al. [34]. They indicated an average thermal and electrical efficiency of 22% and

15%, respectively. The results of this study show that with a low-cost absorber plate, a higher thermal efficiency can be achieved. Tonui and Tripanagnostopoulos [23] evaluated an unglazed air PV/T system with an aluminum air channel of 0.15 (m) in depth. The thermal and electrical efficiencies were reported as 18% and 12% with the mass flow rates of 0.05 (kg/s.m²). All the systems mentioned above were the unglazed types of PV/Ts. The glazed ones with a glass cover have more thermal efficiency. The single channel glazed air PV/T system studied by Amori and Abd-AllRaheem [35] had a copper absorber plate and an air channel with 0.24 (m) depth. At the midday, the thermal and electrical efficiencies were obtained as 50% and 10%, respectively.

The values obtained for the electrical output in Fig. 11 are shown without considering the amount of the fan power. The amounts of heat and electrical power produced by the PV/T system are compared with the fan power requirement for different mass flow rates in Fig. 15. The diagram is plotted for the channel depth of 5 (cm). The trend is same as the other channel depths. By increasing the air flow rate, the power consumption of fans increases. Increasing the mass flow rate improves the thermal power, cooling of PV panels and produces more power of photovoltaic panels compared to free convection. On the other hand, the electrical energy consumption by fan reduces the electrical efficiency. Increasing the mass flow rate causes enhancement of the fan power consumption from 1.5 (W) to 19.25 (W) and thermal energy from 167 (W) to 320 (W), while the electrical power is not changed noticeably. By considering the electrical energy consumption of the fan in the calculations of electrical efficiency, the electrical efficiency somehow decreases with increasing the mass flow rate. But the point is that the increase in the thermal gain is much more than the decrease of electrical efficiency, the gained heat completely compensates the electrical consumption. The obtained extra heat could be consumed in the heating processes such as space heating. Also, the Electrical efficiency in the case of considering the electrical energy consumption of the fan for various mass flow rates is indicated in Fig. 16. As shown in the Fig. 16., the lowest mass flow rate has the highest electrical efficiency.

So, the maximum electrical efficiency can be achieved by the optimal amount of air flow rate. In continue, the optimum mass flow can be determined by simulation and optimization of the system. The fans in this air PV/T system are connected to the duct of PV panel. It should be noted that, with proper hydraulic design, the pressure drop and the input electrical energy can be reduced.

6. Conclusion

This paper deals with implementing an experimental procedure to evaluate the performance of a hybrid PV/T collector system for the insolation and weather condition of Tehran. In this

case, the attempt is to enhance the performance of the air-cooled PV/T by manufacturing a low-cost prototype. Therefore, the steel absorber plate is applied, and aluminum oxide paste is used for sticking the plate to PV panels. The effect of parameters including air mass flow rate and depth of the channel were tested. The following results were obtained:

The daily thermal and electrical efficiencies reached 35% and 12.2%, respectively. These efficiencies have been achieved for the channel depth of 0.05 (m) and air mass flow rate of 0.06 (kg/s). The change in the channel depth does not have a significant effect on the electrical efficiency. However, decreasing the channel depth increases the thermal efficiency. Variation of the channel depth from 0.15 to 0.05 (m) causes 20% increment of the overall efficiency. The thermal and electrical efficiencies improve with increasing air mass flow rate. In fact, changing the mass flow rate from 0.018 (kg/s) to 0.06 (kg/s) resulted in variation of the average thermal and electrical efficiency in the range of 15%-31% and 12%-24%, respectively.

Acknowledgment

The fourth author would like to thank King Mongkut's University of Technology Thonburi for Postdoctoral fellowship during his research in Thailand. The fifth author acknowledges the financial support provided by the "Research Chair Grant" National Science and Technology Development Agency (NSTDA), the Thailand Research Fund (TRF), the National Research University Project (NRU) and King Mongkut's University of Technology Thonburi through the "KMUTT 55th Anniversary Commemorative Fund".

References

1. Shan, F., et al., *Performance evaluations and applications of photovoltaic-thermal collectors and systems*. Renewable and Sustainable Energy Reviews, 2014. **33**: p. 467-483.
2. Chow, T.T., *A review on photovoltaic/thermal hybrid solar technology*. Applied Energy, 2010. **87**(2): p. 365-379.
3. Ebrahimi, M., M. Rahimi, and A. Rahimi, *An experimental study on using natural vaporization for cooling of a photovoltaic solar cell*. International Communications in Heat and Mass Transfer, 2015. 65: p. 22-30.
4. Karami, N. and M. Rahimi, *Heat transfer enhancement in a hybrid microchannel-photovoltaic cell using Boehmite nanofluid*. International Communications in Heat and Mass Transfer, 2014. 55: p. 45-52.

5. Moradi, K., M. Ali Ebadian, and C.-X. Lin, *A review of PV/T technologies: Effects of control parameters*. International Journal of Heat and Mass Transfer, 2013. **64**: p. 483-500.
6. Aste, N., G. Chiesa, and F. Verri, *Design, development and performance monitoring of a photovoltaic-thermal (PVT) air collector*. Renewable Energy, 2008. **33**(5): p. 914-927.
7. Bambrook, S. and A. Sproul, *Maximising the energy output of a PVT air system*. Solar Energy, 2012. **86**(6): p. 1857-1871.
8. Arcuri, N., F. Reda, and M. De Simone, *Energy and thermo-fluid-dynamics evaluations of photovoltaic panels cooled by water and air*. Solar Energy, 2014. **105**: p. 147-156.
9. Hussain, F., et al., *Design development and performance evaluation of photovoltaic/thermal (PV/T) air base solar collector*. Renewable and Sustainable Energy Reviews, 2013. **25**: p. 431-441.
10. Kumar, R. and M.A. Rosen, *A critical review of photovoltaic-thermal solar collectors for air heating*. Applied Energy, 2011. **88**(11): p. 3603-3614.
11. Zondag, H.A., *Flat-plate PV-Thermal collectors and systems: A review*. Renewable and Sustainable Energy Reviews, 2008. **12**(4): p. 891-959.
12. Michael, J.J., I. S, and R. Goic, *Flat plate solar photovoltaic-thermal (PV/T) systems: A reference guide*. Renewable and Sustainable Energy Reviews, 2015. **51**: p. 62-88.
13. Yang, T. and A.K. Athienitis, *A review of research and developments of building-integrated photovoltaic/thermal (BIPV/T) systems*. Renewable and Sustainable Energy Reviews, 2016. **66**: p. 886-912.
14. Slimani, M.E.A., et al., *A detailed thermal-electrical model of three photovoltaic/thermal (PV/T) hybrid air collectors and photovoltaic (PV) module: Comparative study under Algiers climatic conditions*. Energy Conversion and Management.
15. Farshchimonfared, M., J.I. Bilbao, and A.B. Sproul, *Full optimisation and sensitivity analysis of a photovoltaic-thermal (PV/T) air system linked to a typical residential building*. Solar Energy, 2016. **136**: p. 15-22.
16. Hazami, M., et al., *Energetic and exergetic performances analysis of a PV/T (photovoltaic thermal) solar system tested and simulated under to Tunisian (North Africa) climatic conditions*. Energy, 2016. **107**: p. 78-94.
17. Hou, L., et al., *An experimental and simulative study on a novel photovoltaic-thermal collector with micro heat pipe array (MHPA-PV/T)*. Energy and Buildings, 2016. **124**: p. 60-69.
18. Khanjari, Y., F. Pourfayaz, and A.B. Kasaeian, *Numerical investigation on using of nanofluid in a water-cooled photovoltaic thermal system*. Energy Conversion and Management, 2016. **122**: p. 263-278.
19. Good, C., *Environmental impact assessments of hybrid photovoltaic-thermal (PV/T) systems – A review*. Renewable and Sustainable Energy Reviews, 2016. **55**: p. 234-239.

20. Romero Rodríguez, L., et al., *Analysis of the economic feasibility and reduction of a building's energy consumption and emissions when integrating hybrid solar thermal/PV/micro-CHP systems*. Applied Energy, 2016. **165**: p. 828-838.
21. Pierrick, H., et al., *Dynamic numerical model of a high efficiency PV-T collector integrated into a domestic hot water system*. Solar Energy, 2015. **111**: p. 68-81.
22. Tiwari, A., et al., *Performance evaluation of photovoltaic thermal solar air collector for composite climate of India*. Solar energy materials and solar cells, 2006. **90**(2): p. 175-189.
23. Tonui, J. and Y. Tripanagnostopoulos, *Air-cooled PV/T solar collectors with low cost performance improvements*. Solar Energy, 2007. **81**(4): p. 498-511.
24. Tonui, J. and Y. Tripanagnostopoulos, *Improved PV/T solar collectors with heat extraction by forced or natural air circulation*. Renewable Energy, 2007. **32**(4): p. 623-637.
25. Raman, V. and G. Tiwari, *Life cycle cost analysis of HPVT air collector under different Indian climatic conditions*. Energy Policy, 2008. **36**(2): p. 603-611.
26. Raman, V. and G. Tiwari, *A comparison study of energy and exergy performance of a hybrid photovoltaic double-pass and single-pass air collector*. International Journal of Energy Research, 2009. **33**(6): p. 605-617.
27. Joshi, A., et al., *Performance evaluation of a hybrid photovoltaic thermal (PV/T)(glass-to-glass) system*. International Journal of Thermal Sciences, 2009. **48**(1): p. 154-164.
28. Solanki, S., S. Dubey, and A. Tiwari, *Indoor simulation and testing of photovoltaic thermal (PV/T) air collectors*. Applied energy, 2009. **86**(11): p. 2421-2428.
29. Ameri, M., M. Mahmoudabadi, and A. Shahsavari, *An Experimental Study on a Photovoltaic/Thermal (PV/T) Air Collector With Direct Coupling of Fans and Panels*. Energy Sources, Part A: Recovery, Utilization, and Environmental Effects, 2012. **34**(10): p. 929-947.
30. Shahsavari, A., M. Ameri, and M. Gholampour, *Energy and exergy analysis of a photovoltaic-thermal collector with natural air flow*. Journal of Solar Energy Engineering, 2012. **134**(1): p. 011014.
31. Jin, G.L., et al., *Evaluation of single-pass photovoltaic-thermal air collector with rectangle tunnel absorber*. American Journal of Applied Sciences, 2010. **7**(2): p. 277.
32. Agrawal, S. and G. Tiwari, *Overall energy, exergy and carbon credit analysis by different type of hybrid photovoltaic thermal air collectors*. Energy conversion and Management, 2013. **65**: p. 628-636.
33. Ji, J., et al., *Experimental investigation of tri-functional photovoltaic/thermal solar collector*. Energy Conversion and Management, 2014. **88**: p. 650-656.
34. Kim, J.-H., S.-H. Park, and J.-T. Kim, *Experimental Performance of a Photovoltaic-thermal Air Collector*. Energy Procedia, 2014. **48**: p. 888-894.
35. Amori, K.E. and M.A. Abd-ElRaheem, *Field study of various air based photovoltaic/thermal hybrid solar collectors*. Renewable Energy, 2014. **63**: p. 402-414.

36. Sarhaddi, F., et al., *An improved thermal and electrical model for a solar photovoltaic thermal (PV/T) air collector*. Applied Energy, 2010. **87**(7): p. 2328-2339.

ACCEPTED MANUSCRIPT

Table 1. Properties of the PV panels

Peak power	P_{\max}	[Wp]	90
Max. power current	I_{mp}	[A]	5.47
Max. power voltage	V_{mp}	[V]	16.45
Short circuit current	I_{sc}	[A]	5.55
Open circuit voltage	V_{oc}	[V]	20.2
Temperature coefficient for P_{\max}		[%/°C]	-0.46
Temperature coefficient for V_{oc}		[%/°C]	-0.356
Temperature coefficient for I_{sc}		[%/°C]	+0.024
Max system voltage		[V]	1000

Table 2. Properties of the monitoring equipment

Equipment	Range	Accuracy
Pyranometer	0 to 2000 Wm^{-2}	$\pm 5\%$
Hot wire anemometer	0.2 to 20.0 m/s	$\pm 5\%$
Cup anemometer	0.9 to 35.0 m/s	$\pm 2\%$
Thermometer (type K)	-199.9 to 999.9 °C	$\pm 0.5\%$
SMT 160 sensor	-45 to 150 °C	$\pm 0.7\%$
Multimeter DC voltage	400mV/4V/40V/400V/1000V	$\pm 0.5\%$
Multimeter DC current	400 μA /4mA/40mA/400mA/10A	$\pm 0.8\%$

Table 3. The measured parameters (in channel depth of 5 (cm), tilt angle of 35° and mass flow rate of 0.06 (kg/s))

Time	T _a (°C)	V _w (m/s)	T _{in} (°C)	T _{out} (°C)	T _{topPV} (°C)	T _{abs} (°C)	T _{bs} (°C)	I _{sc} (A)	V _{oc} (V)	I _{mp} (A)	V _{mp} (V)	G (W/m ²)
9:00	33.00	0.9	34.27	36.70	38.18	39.98	44.10	3.19	36.62	2.21	33.56	512.55
9:30	32.91	2.0	34.27	37.07	39.42	41.64	45.50	3.56	36.46	2.67	31.44	596.69
10:00	33.55	2.0	34.39	37.91	40.62	44.00	47.04	3.76	36.30	3.20	32.49	702.68
10:15	34.12	2.5	34.92	38.47	42.67	45.33	48.80	3.96	36.08	3.27	33.02	747.53
10:45	34.58	2.5	35.79	40.19	45.20	48.56	53.08	4.14	35.86	3.68	31.66	835.55
11:15	34.99	2.5	35.57	40.85	47.09	50.98	56.69	4.57	35.42	3.81	31.67	903.80
11:45	34.55	3.3	34.93	40.16	46.90	50.47	56.08	5.04	35.70	3.95	32.16	962.23
12:15	34.50	3.0	35.29	40.78	47.91	51.31	56.70	5.24	35.52	4.23	31.46	1008.48
12:45	35.17	2.5	35.30	41.07	49.10	53.18	57.89	5.3	35.30	4.44	30.53	1015.43
13:15	35.81	3.5	35.97	42.06	51.43	54.43	59.30	5.26	35.60	4.48	30.50	1016.11
13:45	36.66	2.4	36.55	42.91	53.57	55.80	60.76	5.23	35.40	4.45	30.38	1005.12
14:00	36.79	2.4	36.99	43.09	51.96	56.13	61.50	5.09	35.30	4.41	30.34	978.54
14:30	36.73	3.5	36.81	42.57	51.71	54.27	60.82	4.62	35.26	4.12	30.82	936.41
15:00	36.85	3.5	37.25	42.79	49.53	53.90	58.98	4.37	35.44	3.94	31.66	884.09
15:30	37.85	2.3	37.92	42.55	49.30	51.67	56.50	3.95	35.34	3.66	31.25	803.92
16:00	37.48	2.1	38.04	41.74	47.41	50.51	54.68	3.57	35.60	3.21	32.33	708.80
16:30	37.09	2.1	37.88	41.23	44.43	46.74	52.58	3.18	35.88	2.66	32.74	615.72
17:00	37.45	2.3	38.20	40.95	42.65	44.49	48.64	2.95	35.80	2.38	32.29	535.16

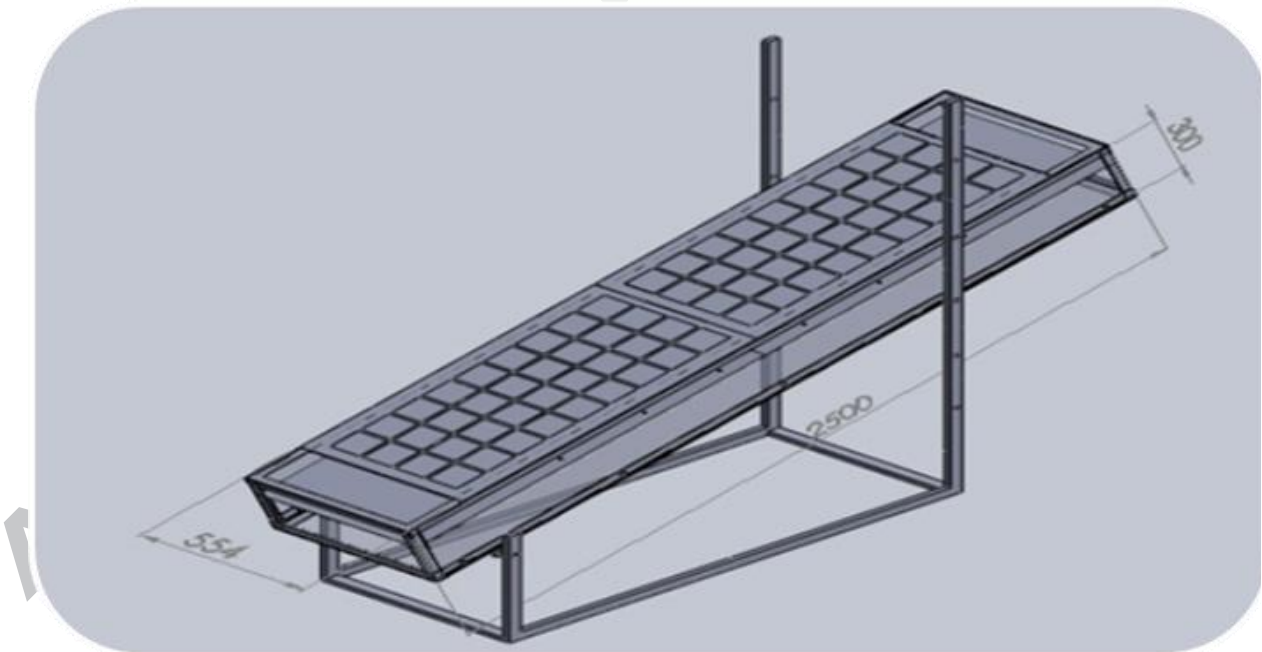
*a**b*

Fig. 1. (a) A photograph of experimental setup of hybrid PV/T air collector (b) A schematic of experimental setup

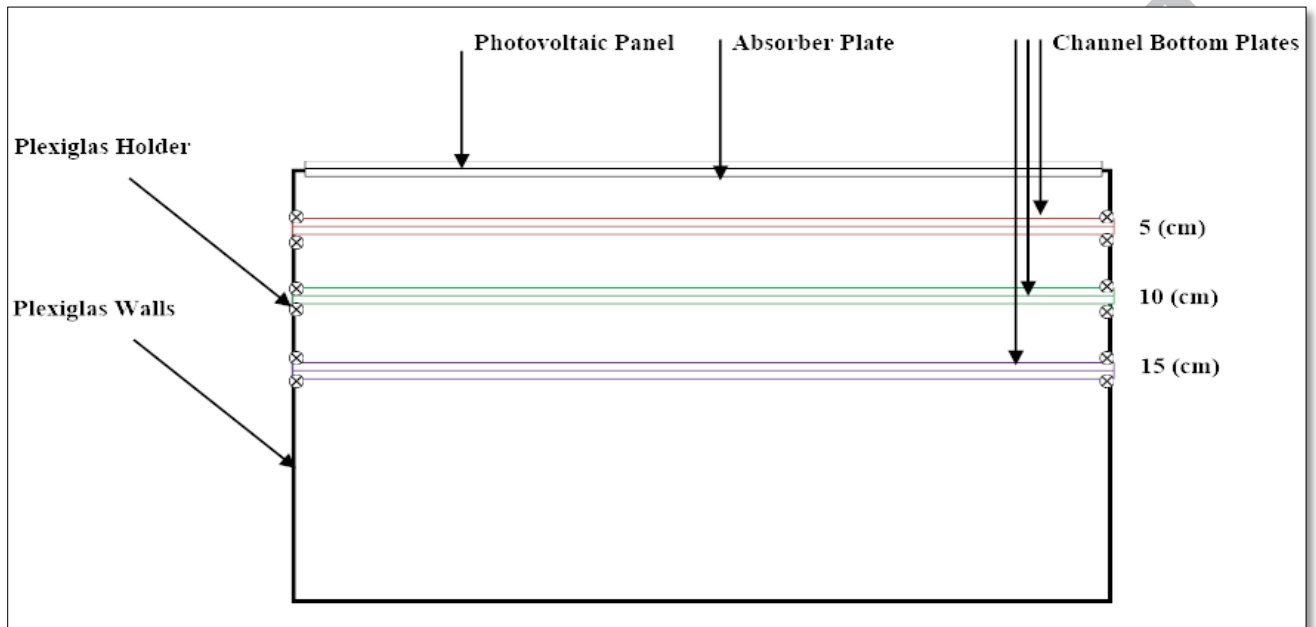


Fig. 2. Channel depth adjustment positions in the set up

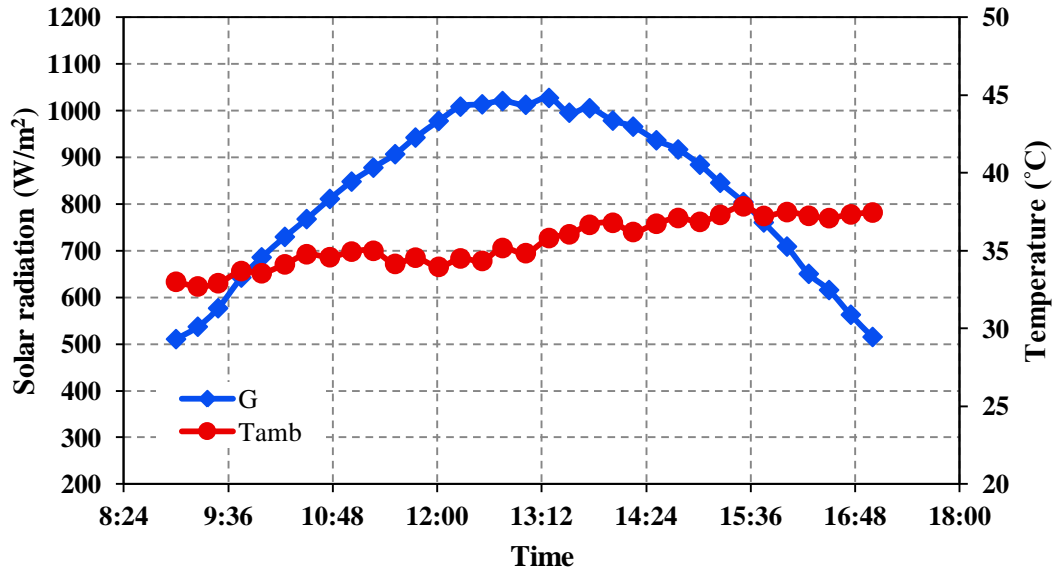


Fig. 3. Hourly variations of solar intensity and ambient temperature on 10thSeptember, 2013.

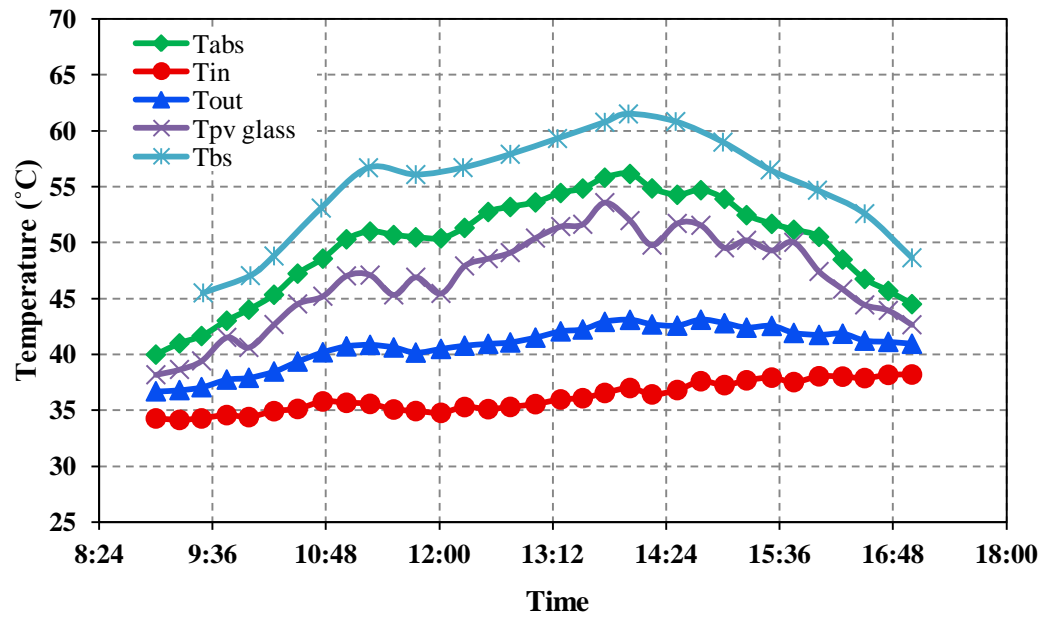


Fig. 4. Hourly temperature variation of different sections

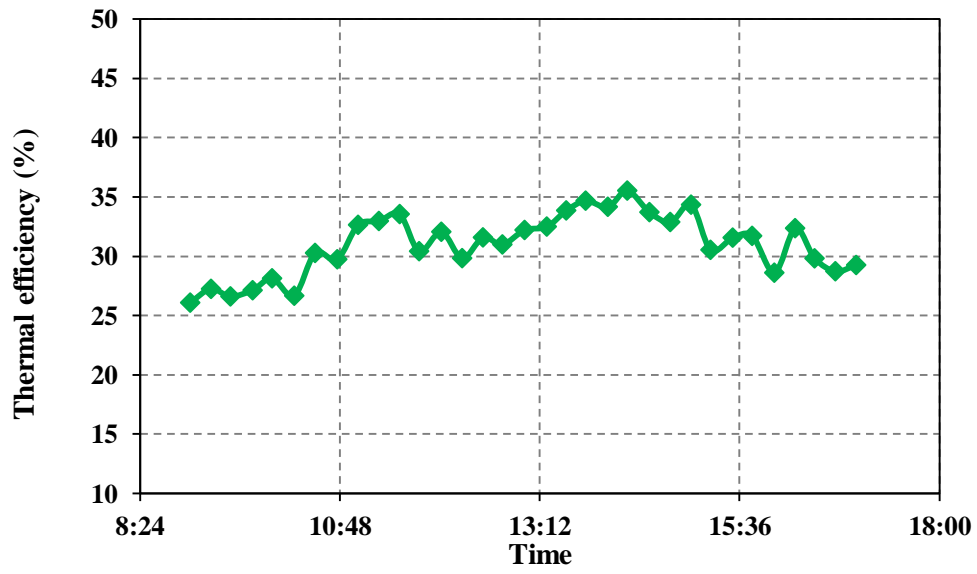


Fig. 5. Variations of thermal efficiency versus time

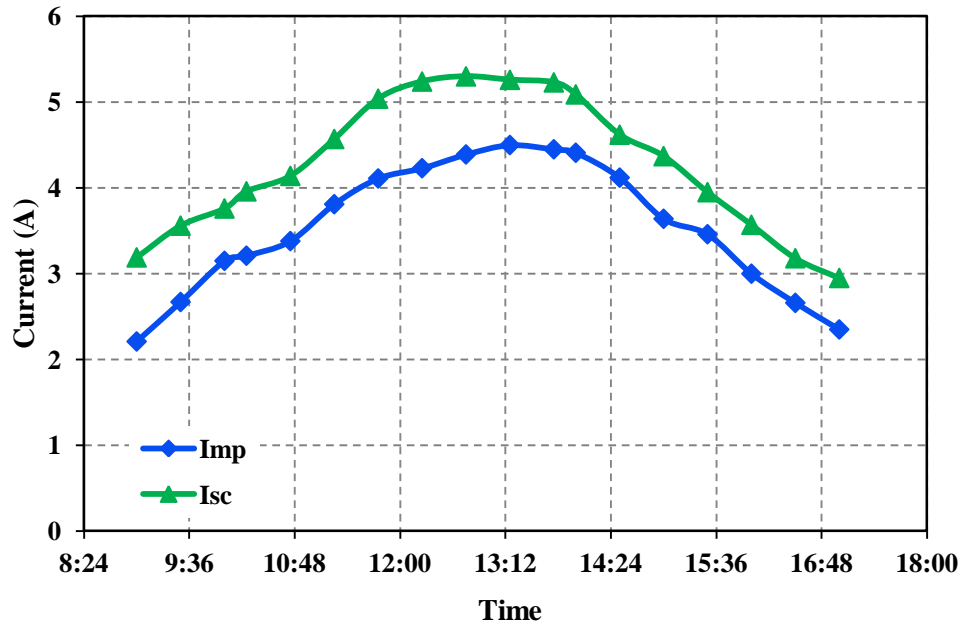


Fig. 6. Variations of short circuit current and the current in the maximum power output versus time

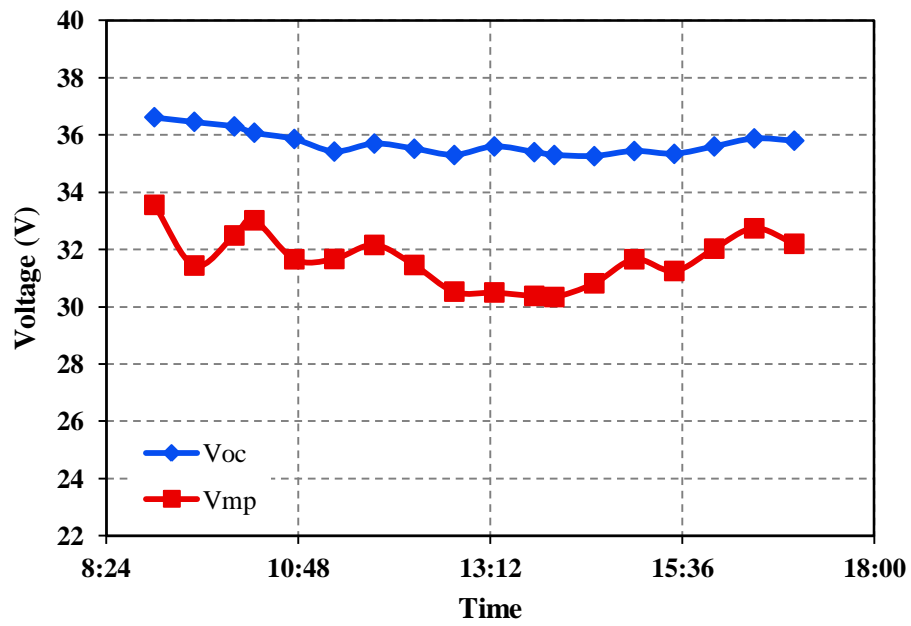


Fig. 7. Variations of open circuit voltage and the voltage in the maximum power output versus Time

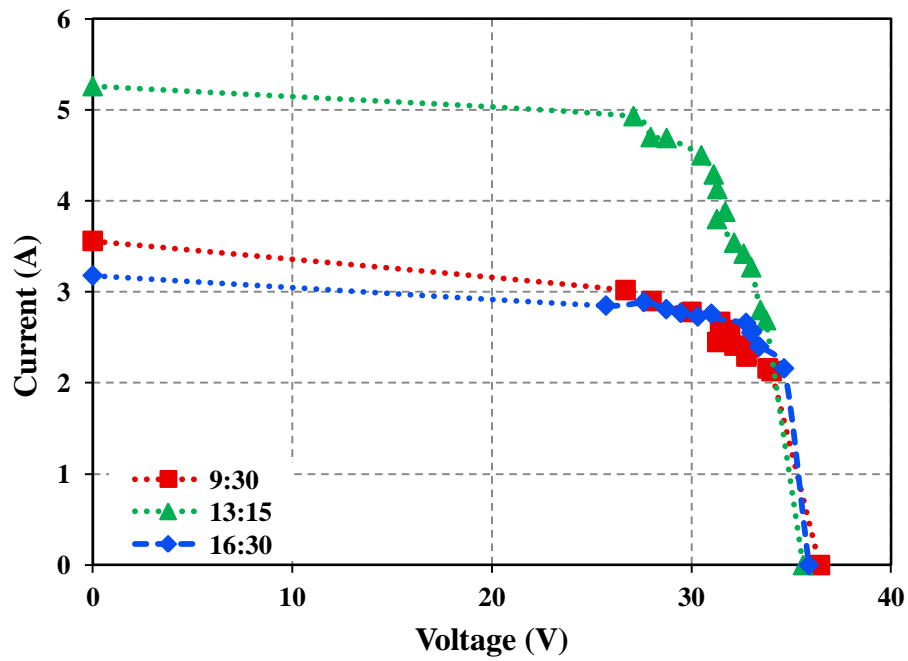


Fig. 8. The I-V characteristic curves of solar panels in three different hours

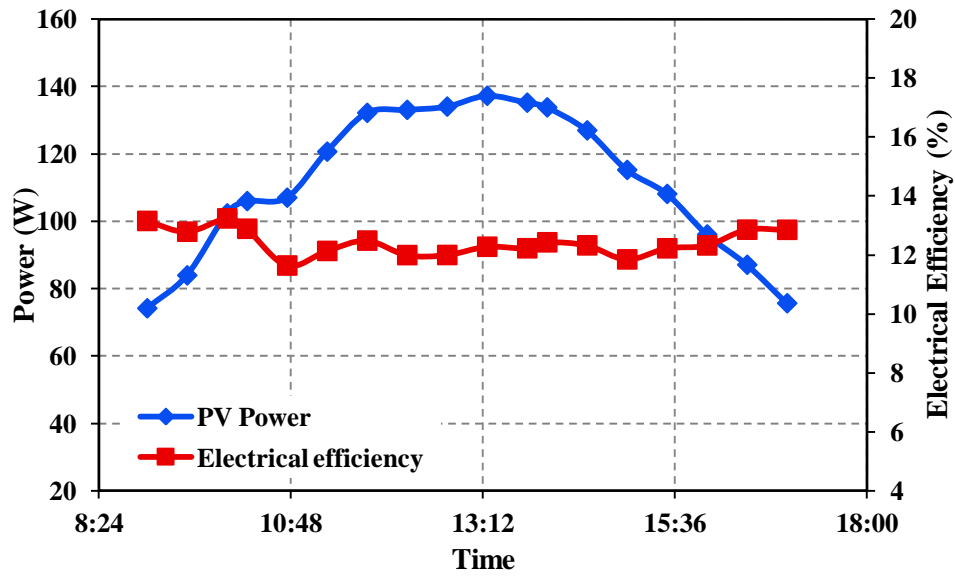


Fig. 9. The variation of power generation and electrical efficiency of photovoltaic panels versus time

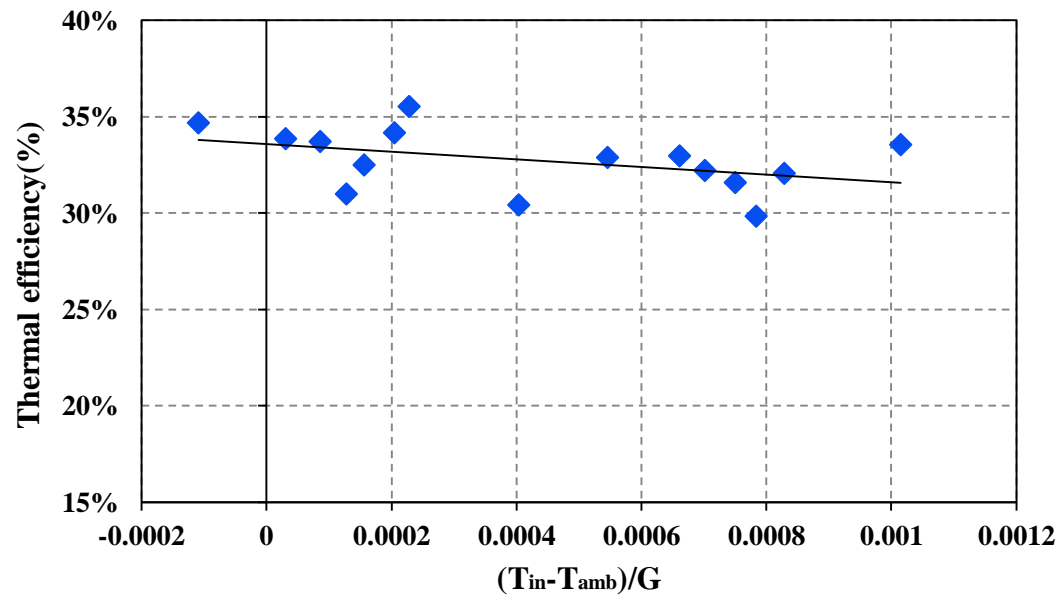


Fig.10. Thermal efficiency of the PV/T system versus reduced temperature

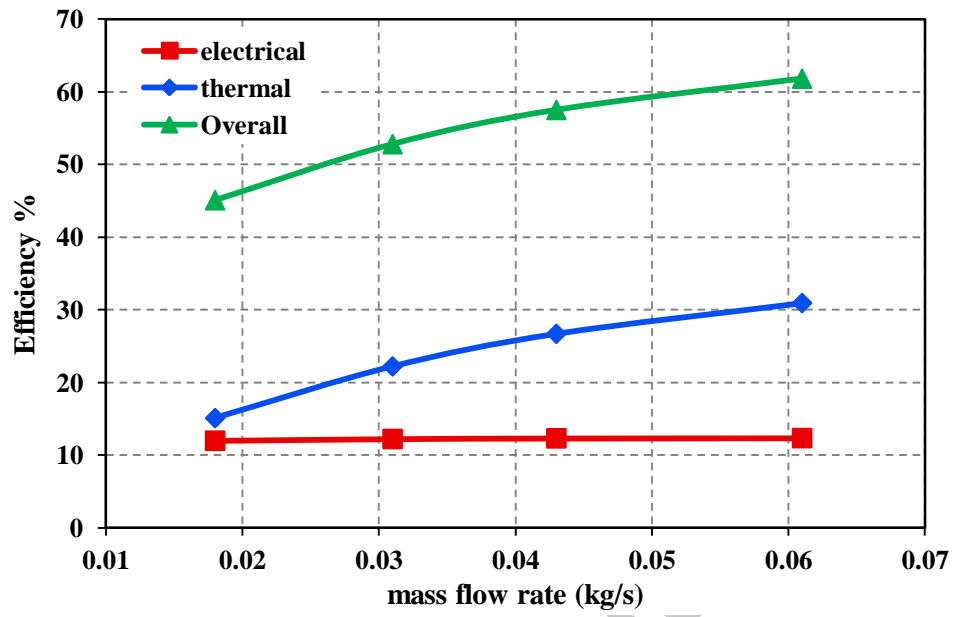


Fig. 11. Variations of electrical, thermal and overall efficiencies in the channel versus mass flow rate

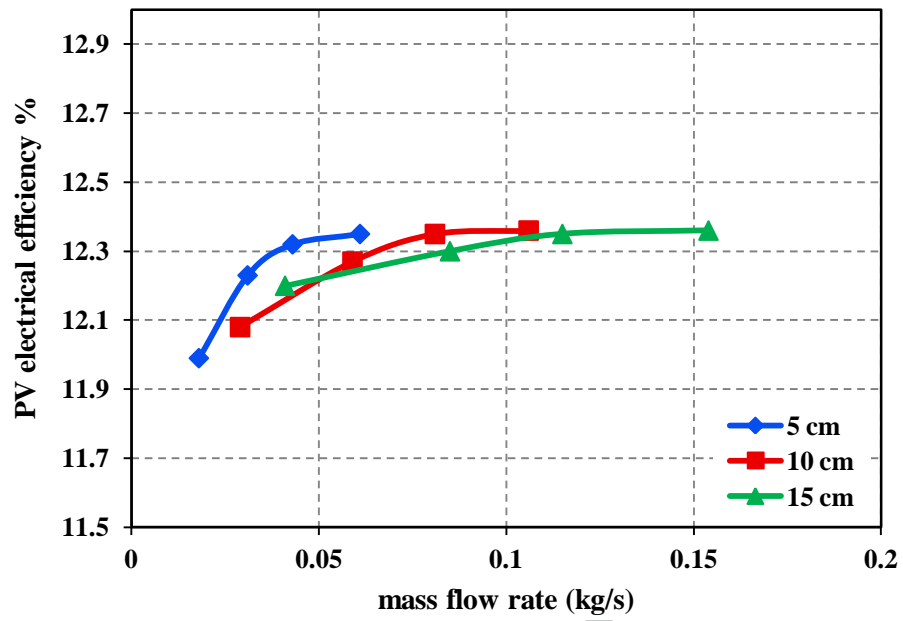


Fig. 12. Variations of the electrical efficiency of photovoltaic panels in different channel depths versus mass flow rate

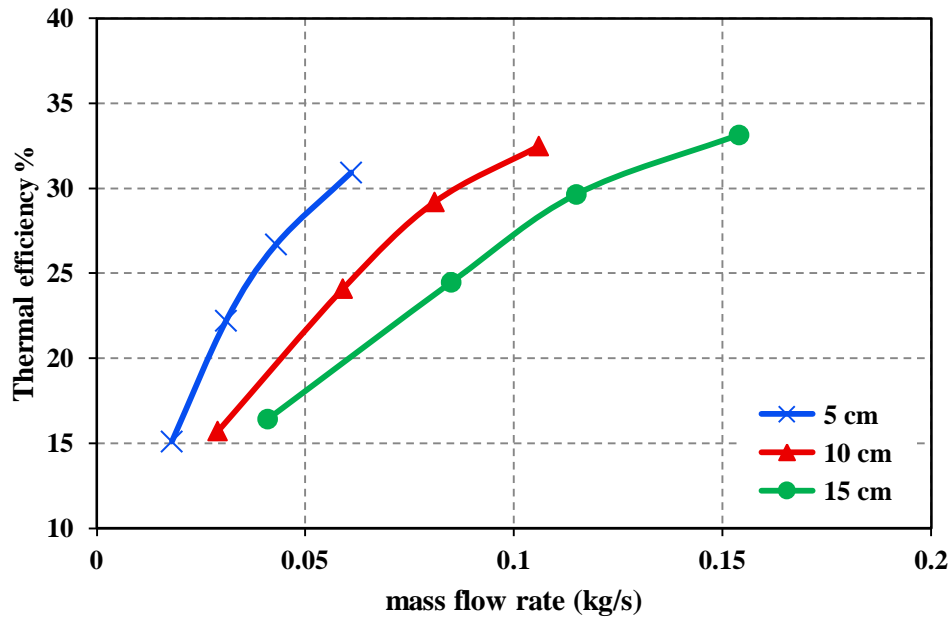


Fig.13. Variations of the thermal efficiency of photovoltaic panels in different channel depths versus mass flow rate

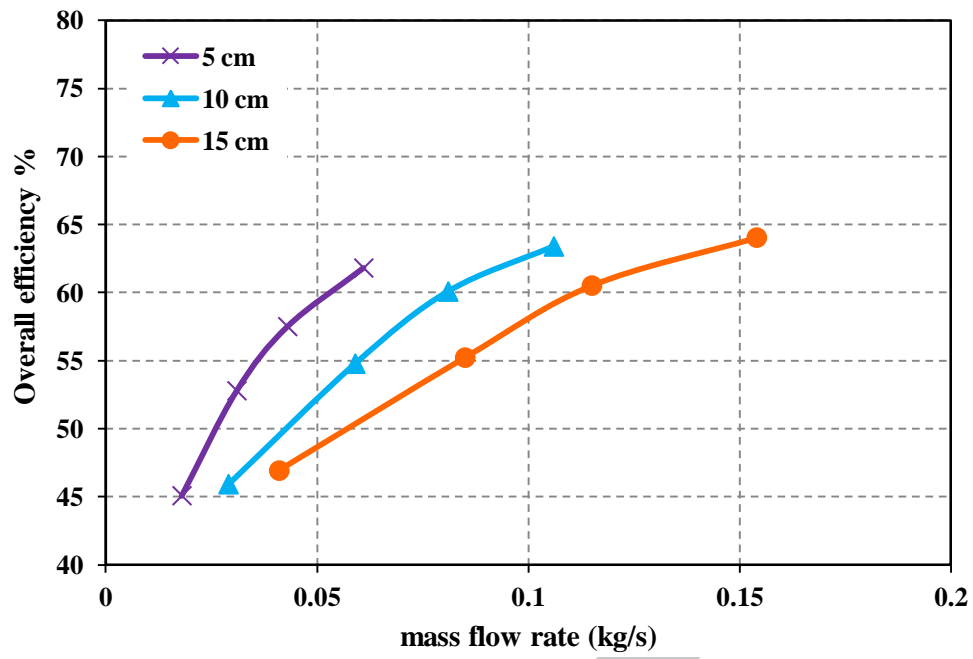


Fig. 14. Variations of overall efficiency versus mass flow rate in different channel depth values

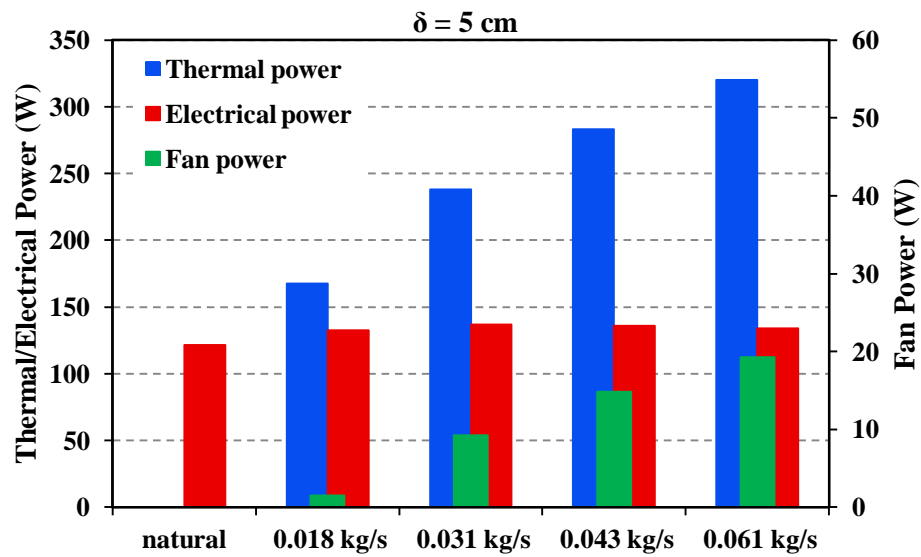


Fig.15. PV/T system energy output and fan power versus air mass flow rate

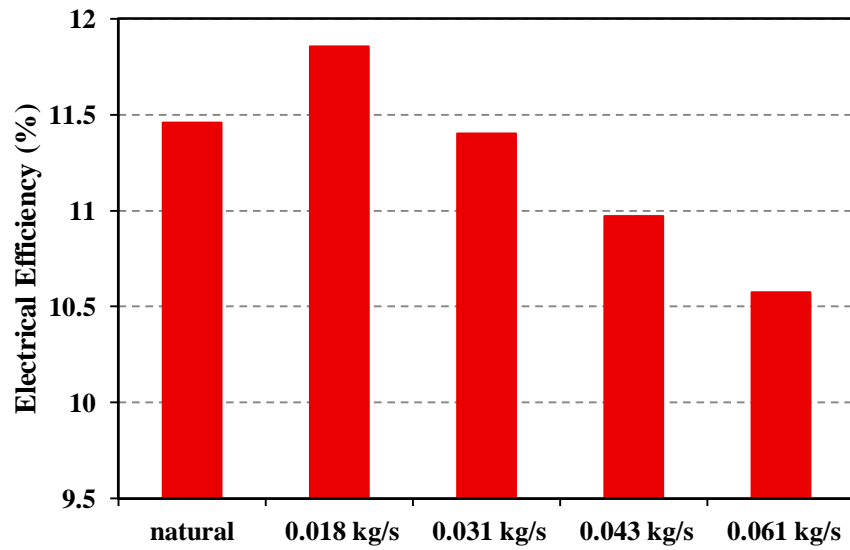


Fig. 16. Electrical efficiency in the case of considering the electrical energy consumption of the fan

Highlights

- A photovoltaic thermal system (PV/T) is a combination of solar cells and solar heating systems .
- The paper investigates the effects of forced convection on the thermal and electrical efficiencies of a PV/T system.
- The reduction in the depth of channel increases the thermal efficiency, but no effect on the electrical efficiency.
- With increasing the Reynolds number , the thermal efficiency is increased,
- The thermal efficiency of system is in the range of 15–31% while the electrical efficiency changes in the range of 12-12.4%.